IEEE Access
Multidisciplinary | Rapid Review | Open Access Journal

Received May 16, 2019, accepted June 3, 2019, date of publication June 12, 2019, date of current version June 26, 2019.

Digital Object Identifier 10.1109/ACCESS.2019.2922203

PSO-Based Dynamic UAV Positioning Algorithm for Sensing Information Acquisition in Wireless Sensor Networks

HO JEONG NA AND SANG-JO YOO, (Member, IEEE)
Department of Information and Communication Engineering, Inha University, Incheon 402-751, South Korea

Corresponding author: Sang-Jo Yoo (sjyoo@inha.ac.kr)

This research was supported by the Basic Science Research Program through the National Research Foundation of Korea (NRF) funded by the Ministry of Science and ICT under Grant 2017R1A2B4003512.

ABSTRACT In this paper, we propose a dynamic unmanned aerial vehicle (UAV) positioning method to maximize the value of the sensor data information acquired from multiple UAVs in wireless sensor networks. In operations of UAVs to monitor environmental disasters or perform military missions, the value of the acquired sensing information depends on the sensor types and the elapsed time after the previous sensing time. To support real-time sensor data monitoring, the sensed data should be successfully delivered to the ground base station (or sink node) using a UAV flying ad-hoc network; herein, it is important to maintain the connectivity between the UAVs and to consider the reliability of the communication links. In this paper, particle swarm optimization (PSO) is used to derive optimum UAV locations. For a specified wireless sensor network, at each time instance, new UAV locations are updated that guarantee complete connectivity of the UAVs and maximize the value of the aggregated sensor data information. In this paper, we have formulated the UAV location search model as a constrained optimization problem with multi-objective utility functions using PSO-based bio-inspired algorithm. The simulation results demonstrate that by maximizing the intended multi-objective utility function, the proposed method can dynamically derive the optimal locations of multiple UAVs and achieve better sensing information acquisition compared to other methods.

INDEX TERMS UAV, wireless sensor networks, positioning, bio-inspired algorithm, particle swarm optimization.

I. INTRODUCTION

Recently, unmanned aerial vehicles (UAVs) have been widely applied to numerous areas including environment monitoring, mission critical military operations, leisure, delivery of goods, security and surveillance, precision agriculture, and remote sensing [1]–[4].

In particular, UAVs can be used successfully in wireless sensor networks (WSNs), in which sensor nodes are deployed in a relatively wide region and multiple UAVs acquire sensed information. Then, the information obtained by each UAV is delivered to a sink node or ground base station (GBS) using a UAV flying ad-hoc network (FANET). In conventional WSNs, each sensor node delivers their monitored data to a sink node via multi-hop transmissions, in which sensor nodes need to not only transmit their sensed data but also relay the other's. As a result, sensors' battery may drain quickly and sensor network can be partially disconnected. Therefore, to collect sensor data more effectively, UAV-assisted sensor networks have been considered as a promising technology to extend network life time, expand network coverage and provide a faster and reliable data collecting. UAVs are also very useful to deploy sensors and acquire their data especially in disaster scenarios. Costa *et al.* [4] adjust the UAV route based on the feedback information from sensors deployed on a crop field, to minimize pesticide wastage. UAVs can play an important role in natural disaster management, e.g., monitoring and predicting [5] when humans are unable to enter a disaster area; moreover, they can improve the monitoring performance when the communication links between sensors in a sensor network are unreliable owing to weak signals or relay node failure [6]. In addition, in [7], a study using UAVs to deploy WSNs to monitor areas damaged by disasters have been conducted. Dong *et al.* [8] studied the efficient use of

The associate editor coordinating the review of this manuscript and approving it for publication was Gerhard P. Hancke.

a UAV's energy in an environment where it acquires sensor data from a large number of sensors. Because a number of sensor nodes send their data to the UAV, the energy consumption of the UAV is large. Therefore, in order to reduce the data concentrated in the UAV, a mobile agent (MA) is used to collect the data of each corresponding area; moreover, the UAV obtains the desired information through the MA. The simulation results of this study demonstrate that the time and energy required to obtain sensor data under different network conditions can be reduced.

Although numerous studies have used UAVs to collect sensor data, it is inconvenient and occasionally infeasible for UAVs to acquire sensor data from all the deployed sensors because of the sensors' random placement in a large area; moreover, the inadequate battery power of UAVs limits their operation time. Of particular importance in optimizing the energy consumption and fast sensor data acquisition of the UAV network is the UAV positioning or trajectory generation. Due to the energy and time limits, UAVs are not able to search the entire WSN area. To maximize the objective function of the given application at each UAV movement and maintain the UAV FANET connectivity at time same time, the optimum positions UAVs should be carefully considered.

In this study, different types of sensors are deployed in a wide area, where the values of the data sensed by different sensor types could be different. We assume that the sensor deployment topology and three-dimensional (3D) geographical map are obtained in advance. The objective of our study is to identify the UAV positions where the value of the sensed data can be maximized by considering the different sensing information values, which depend on the sensor type and previously acquired sensor data, the UAV connectivity, and the location-dependent communication link quality. To derive real-time dynamic optimal UAV positions, we use the particle swarm optimization (PSO) algorithm; in this algorithm, a particle represents candidate multiple-UAV locations. In the proposed PSO algorithm, we have defined a multi-objective utility function that incorporates the UAV connectivity, sensing information value, and communication path quality. By applying PSO at each UAV position-readjustment time, new multiple-UAV locations are determined. Once sensor data is obtained from the new positions, the sensing information value functions for the different sensor types are updated based on the sensing data acquisition history.

This paper is organized as follow: In Section 2, we review the available research on the application of UAVs in WSNs. In Section 3, the proposed system model is presented. The multi-objective utility function for evaluating each particle in the PSO algorithm is described in Section 4. The proposed optimal location search method using PSO algorithm is presented in Section 5. The simulation results are presented in Section 6. The conclusions are presented in Section 7.

II. RELATED WORK

Notwithstanding the substantial interest in UAVs, studies on aspects such as location and path planning of UAVs are still in progress. These studies differ in the objective function and optimization method because they assume varied environments. Zhang *et al.* [9] presented a UAV path planning method based on ant colony optimization (ACO). First, the UAV flight area is divided into grids, and the shortest distance between the radar and the flight path segment is considered as the threat intensity. Then, the ACO algorithm is used to optimize the path between the starting point and destination point. The weighted sums of the flight path length, threat cost, and maximum restriction of the yaw angle are considered as the evaluation function of the ACO algorithm. Mittal and Deb [10] presented a 3D offline path planner for UAVs using multi-objective evolutionary algorithms for determining solutions corresponding to the conflicting objectives of minimizing the path-length and maximizing the margin of safety. They used the NSGA-II algorithm to generate a curved path expressed using a B-spline and addressed cases where there were no constraints and there were areas that to be pass. Mishra *et al.* [11] modeled a coordinated path planning problem for a team of UAVs within a dynamic mission scenario; here, the UAVs were required to cooperatively execute time-critical mission tasks in the presence of a manned aircraft. The purpose of their study was to synchronize the UAVs' arrival time while allowing for loitering en-route to prevent collisions and for maintaining a safe distance from the manned aircraft or other obstacles. In another study [12], the path planning of multiple UAVs by using a genetic algorithm (GA) is presented; the path was smoothed using Bezier curves.

In addition to the researches on UAV flying route planning wherein a UAV moves from a starting point to a destination, there are researches to determine a strategy of UAV and sensors for acquiring sufficient amount of data reliably in a specified WSN environment. Ho *et al.* [13] addressed the selection of sensor network communication topology for data gathering with UAV. The topology consisted of a set of cluster heads that communicate with the UAV; moreover, PSO is proposed as an optimization method to determine the optimal topology in order to reduce the energy consumption, bit error rate (BER), and UAV travel time. Ergezer and Leblebicioglu [14] proposed a method for path planning of UAV that can evade prohibited areas, maximize information collection in the desired area, and reach the destination in a fixed mission time by using the GA algorithm. However, they did not consider the link quality; moreover, the searched path planning is for only one UAV. Yang and Yoo [15] presented an optimal flight path planning mechanism using a multi-objective bio-inspired algorithm based on environmental information such as forbidden areas, geographical location conditions, flight risk, and sensor deployment statistics. They defined data acquisition points in an entire sensor field, in which an UAV communicates with sensors to obtain sensor data. Then, they derived the best flight path between neighboring acquisition points. The optimal path is selected according to the sensing, energy, time, and risk utility by using an algorithm

combining GA and ant colony optimization (ACO). Although this study considered multiple objective functions for various constraint environments, it assumed an operation case with one UAV.

There are some researches on framework and mechanisms for efficient and reliable sensor data collection using UAVs. Say *et al.* [16] proposed a priority-based data gathering framework in UAV-assisted WSNs, in which sensors inside the UAV's coverage are divided into different frames having different priorities. For the sensors within the urgent area, higher priority is given. The contention window size is adjusted for each frame. This framework can minimize the number of redundant data transmissions and also provide reliable data acquisition by UAV. Zhan *et al.* [17] jointly optimized the sensor node's wakeup schedule and UAV's trajectory to minimize the maximum energy consumption of all sensor nodes while ensuring that a target amount of sensor data is collected reliably. Zhan *et al.* [18] presented UAV trajectory design to collect the data from any many sensor nodes as possible. They proposed a greedy algorithm with low complexity based on traveling salesman problem (TSP) method and convex optimization to obtain a suboptimal trajectory solution. Gong *et al.* [19] aimed minimizing the UAV's total flight time from a starting point to destination which allowing each sensor to successfully upload a certain amount of data using a given amount of energy. In their research, the data collection interval, UAV's speed, and sensor's transmit power are jointly optimized.

Sánchez-García *et al.* [20] proposed a solution for efficiently generating trajectories for a UAV network in a search mission for a disaster scenario using PSO algorithm, in which it aims to explore the scenario, discover as many victims as possible and converge towards one of the victim cluster. Wang *et al.* [21] proposed a three-dimensional path planning for UAV based on improved PSO algorithm. For UAV path planning, they considered three aspects of fuel, threat and flight altitude. Li *et al.* [22] applied VND (Variable Neighborhood Descend) enhanced Genetic-PSO algorithm to optimize the flight paths for a group of multiple agricultural UAVs, in which the objective is to minimize make-span (i.e., find the optimum path that minimizes the time difference between the start and finish of a sequence of jobs).

In this paper, we propose a dynamic multiple UAV positioning method to maximize the value of sensor data over time by using PSO bio-inspired algorithm in a WSN. Especially, while previous PSO-based approaches have focused on UAV constraints, such as flight distance or flight time of UAVs, we focus on efficient and reliable data acquisition of sensors using UAVs. The proposed method can be performed in an environment in which various types of sensors are deployed and we consider that the value of the acquired sensor data can be changed depending on the sensor type and on when the previous sensor data was obtained (i.e., the freshness of the acquired data).

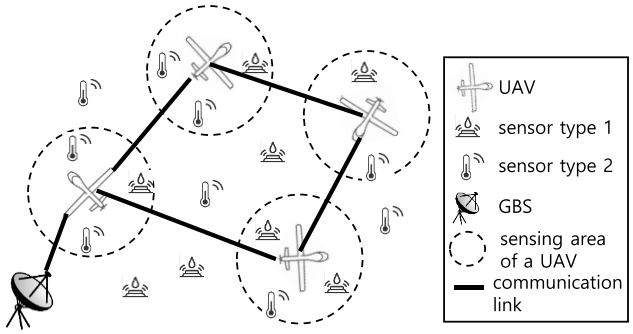

FIGURE 1. System model.

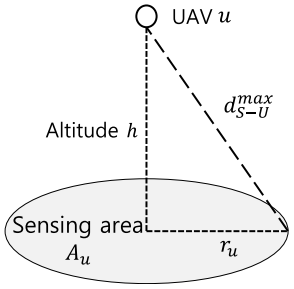

FIGURE 2. Sensing area of UAV.

III. SYSTEM MODEL

In this study, we assume that numerous types of sensors are deployed in a wide area sensor field and that multiple UAVs are used to acquire sensor data in real-time, as shown in Fig. 1. Different types of sensors periodically sense the environment and transmit the sensed data to the UAV (or UAVs) within the communication range. As shown in Fig. 1, the sensed data acquired by each UAV is forwarded to its neighbor UAVs using FANET and eventually delivered to the GBS. It is also assumed that the sensor topographical map is specified prior to the proposed UAV operation; here, the map includes sensor deployment location information and location-dependent expected communication link quality between the UAV and sensors.

In this study, the sensing area of each UAV (shown in Fig. 1) is defined as the ground area in which sensors can communicate with the UAV when it is at a specified location. The sensing area of a UAV (A_U) is determined by the sensing area radius (r_U) as $A_U = \pi r_U^2$; here, r_U can be calculated using the UAV altitude (h) and the maximum communication distance (d_{S-U}^{max}) between a UAV and a sensor (Fig. 2). We assume that all the UAVs maintain a predetermined altitude h while acquiring sensor data from the sensors. It should be noted that owing to the limited battery power of the sensors, the UAVs may be required to maintain a lower altitude while communicating with the sensors than that while flying between positions. When the UAVs vary their location, their flying altitudes can be dynamically determined depending on the geo-location conditions. Related with the optimal UAV altitude h, [23] presented an analytical solution to provide maximum radio coverage on the ground, in which

the optimum h is a function of the maximum allowed pathloss and of the statistical parameters of the urban environment. In [24] for the 5G base stations mounted on aerial platforms, the optimum altitude of aerial base station (ABS) was evaluated from the maximum cell coverage obtained using ray tracing simulation results. In [25], representative field trial results on RSRP (Reference Signal Received Power) and SINR (Signal-to-Interference plus Noise Ratio) between UAV and ground devices for different UAV altitudes were presented. For the rural and urban areas, the UAV altitudes that can provide desired performance were studied.

When data is transmitted from a sensor to a UAV, the power is reduced according to the path loss. Assuming that the path loss occurs in free space (path loss exponent = 2) and without fading effects, the power received by the UAV (P_r^U) is expressed as follows in ideal condition:

$$P_r^U = \frac{G_t^S \times G_r^U \times \lambda_S^2}{(4\pi)^2} \left(\frac{1}{d_{S-U}}\right)^2 P_t^s \tag{1}$$

where P_t^s is the transmission power of the sensor. G_t^S, G_r^U,λ_S, and d_{S-U} represent the transmit antenna gain of the sensor, receive antenna gain of the UAV, wavelength of the signal transmitted by a sensor, and distance between the sensor and UAV, respectively. In order to successfully receive data during wireless communication, the received power must be equal to or higher than the minimum decodable power ($P_r^{U,min}$). Therefore, the maximum distance between the UAV and sensor, d_{S-U}^{max}, can be calculated as:

$$d_{S-U}^{max} = \sqrt{\frac{G_t^S \times G_r^U \times \lambda_S^2 \times P_t^s}{(4\pi)^2 \times P_r^{U,min}}} \tag{2}$$

Once the UAV data acquisition altitude h and maximum distance d_{S-U}^{max} are determined, the sensing area of a UAV is determined as:

$$A_U = \pi \left\{ \frac{G_t^S \times G_r^U \times \lambda_S^2 \times P_t^s}{(4\pi)^2 \times P_r^{U,min}} - h^2 \right\} \tag{3}$$

The objective of this study is to determine the optimum positions of multiple UAVs dynamically during their operation time so as to maximize the total value of the acquired sensor information. The contributions of this study are as follows:

- We have defined the value of sensing information (VSI) for each sensor type; here, the VSI of each type can be different in accordance with the current UAV mission. For example, for a fire detection mission in a national park, the sensing information of temperature sensors and frame sensors are more important than that of vibration sensors.
- We consider the duplication effects of the acquired sensing information in terms of temporal and spatial aspects. At a specified location, the VSI depends on its freshness. If UAVs acquire sensing data at a location, similar to that obtained a short time ago, it is not as valuable as the previous sensing. Alternatively, if at a specified location, the sensing data of a certain sensor type has not been acquired for a relatively long time-period, the VSI of the sensor type at that location should be assigned a higher value. In spatial domain duplication, multiple UAVs acquire sensing data from the same sensors when the sensing areas of multiple UAVs overlap partially; in such cases, the sensing values should not be duplicated. Moreover, in a narrow area, if a large number of sensors of the same type send sensing data, the accumulated sensing value should be re-adjusted to capture the spatial redundancy.
- We take into account the effects of connectivity and expected link quality on the finally obtained sensing utility at the GBS. The connectivity between the UAVs should be maintained to deliver the sensed data to the sink node; moreover, the link quality between neighboring UAVs and between UAVs and sensors determines the delivery ratio of the sensed information.
- In a wide sensor field and a scenario wherein the VSI of each sensor type varies dynamically, the optimization of multiple-UAV positions is an NP-hard problem; therefore, in this paper, we propose a PSO-based multi-objective positioning algorithm.
- Compared with the conventional PSO-based UAV path planning methods that considered optimum trajectory of UAVs to minimize path distance or flight time, we applied PSO to dynamically locate UAVs and construct UAV FANET that can maximize the acquired sensor information by defining value of the sensing information.

IV. UTILITY FUNCTION DESIGN FOR DYNAMIC OPTIMAL POSITIONING OF MULTIPLE UAVS TO MAXIMIZE SENSING VALUE

In this section, we design a multi-objective utility function to dynamically derive the optimal locations of multiple UAVs that can maximize the total VSI. The proposed multi-objective utility function consists of sensing utility, communication path quality utility, and network connectivity utility. The optimal positions of multiple UAVs to acquire sensed data from the sensors within each UAV's sensing area maximize the proposed utility function. Once the UAVs obtain the sensed data, the subsequent optimal positions are computed, and all the UAVs shift to the subsequent positions.

A. VALUE OF SENSING INFORMATION

When a UAV acquires sensed data from the sensors within the UAV's sensing area, the VSI of each sensor type can be different depending on the purpose of the UAV operation, as mentioned in Section III. The sensed data from the more important sensor type should have the larger value. In addition, if the sensing data from certain sensors have not been acquired for a relatively long time-period, the VSI of these sensors should be higher than those of the other sensors of

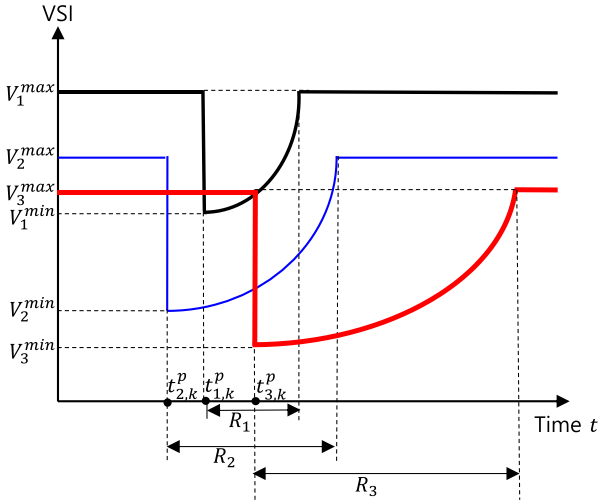

FIGURE 3. Value of sensing information varies over time.

the same sensor type from whom sensing data were acquired recently.

In this paper, for each sensor type j, the initial VSI is defined as $V_j^{init} = V_j^{max}$; once sensing data from a sensor of sensor type j is acquired, the VSI of the sensor is set to V_j^{min}. For any i and j sensor types, if the importance of sensor type i is higher than then that of sensor type j, the following relations hold:

$$V_i^{max} > V_j^{max}, \quad V_i^{min} > V_j^{min} \tag{4}$$

For each sensor type j, a different VSI recovery interval R_j is defined depending on the importance of the sensor type and the required sensing data monitoring interval for the specified application. We define the VSI of sensor k of sensor type j at time t, $v_{j,k}(t)$, as in (5):

$$v_{j,k}(t) = \begin{cases} a \times exp\left(t - t^p_{j,k}\right) + b, & if\ t - t^p_{j,k} \le R_j \\ V_j^{max}, & otherwise \end{cases}$$
$$a = \frac{V_j^{max} - V_j^{min}}{e^{R_j} - 1}, b = V_j^{min} - a \tag{5}$$

where $t^p_{j,k}$ is the time of previous data-acquisition from sensor k of sensor type j.

Fig. 3 shows an example scenario of VSI variations for three sensor types over time using Eq. (5). In this example, $V_1^{max} > V_2^{max} > V_3^{max}$; $V_1^{min} > V_2^{min} > V_3^{min}$; $R_3 > R_2 > R_3$. It is assumed before the each sensor's data acquisition time $t^p_{j,k}$, its VSI value was V_j^{max}. As is evident, when each sensor's sensing data is acquired by UAVs, its VSI decreases to the minimum VSI of all the sensors of its sensor type (V_j^{min}). The sharp decrease in the VSI after sensor data acquisition is to consider the duplication of the time domain. As time elapses, the VSI increases exponentially; furthermore, after the VSI recovery time (R_j), it attains V_j^{max}. After a sensor's VSI attains the maximum value, it is maintained until data from the sensor is again acquired by UAVs.

B. SENSING UTILITY

The sensing utility of UAV u at time t, $U_u^s(t)$, is defined as the total VSI acquired from all the types of sensors within the sensing area of UAV u as follow:

$$U_u^S(t) = \sum_{j=1}^{N_T} U_u^{s(j)}(t) \tag{6}$$

where N_T is the number of sensor types in the entire sensor field and $U_u^{s(j)}(t)$ is the sensing utility of sensor type j acquired by UAV u at time t.

It should be noted that multiple UAVs can obtain sensed data from a sensor when their sensing areas overlap partially and the sensor is located in the overlapped region. In this case, the sensing utility for the sensor can be counted multiple times so that we define the solitary index of each sensor within the sensing area of UAV u at time t as in (7):

$$I^u_{j,k}(t) = \frac{1}{N^U_{j,k}(t)} \tag{7}$$

where $I^u_{j,k}(t)$ is the solitary index of sensor k of sensor type j within the sensing area of UAV u and $N^U_{j,k}(t)$ is the total number of UAVs that can acquire information from sensor k of sensor type j at time t.

In numerous sensor network applications, for a specified area, if the sensor node density is higher than a desired level, the sensed data from the sensors exhibit spatial domain duplication. In this paper, we have defined $U_u^{s(j)}(t)$ as the sensing utility of UAV u for the sensors of type j at time t as in (8):

$$U_u^{s(j)}(t) = c \times log_{10}\left(\frac{\sum_{k=1}^{N_j^u(t)}\left[v^u_{j,k}(t) \times I^u_{j,k}(t)\right]}{d} + 1\right) \tag{8}$$

where $N_j^u(t)$ is the number of sensors of type j within the sensing area of UAV u and $v^u_{j,k}(t)$ is the VSI of sensor k of type j within the sensing area of UAV u. c and d are the constant parameters for determining the desired level of sensing utility. The desired level of $\sum_{k=1}^{N_j^u(t)}\left[v^u_{j,k}(t) \times I^u_{j,k}(t)\right]$ (effective total VSI) for a UAV at a given area is determined by the sensor network operator depending on the operation purpose.

When the threshold x_T (the desired effective total VSI) is set by the operator, the parameter c and d in (8) can be determined to satisfy the following equation. Suppose that $U_u^{s(j)}(t) = \alpha x$ is the reference linear utility function while

$$x = \sum_{k=1}^{N_j^u(t)}\left[v^u_{j,k}(t) \times I^u_{j,k}(t)\right] \cdot c \times log_{10}\left(\frac{x_T}{d} + 1\right) = \alpha x_T \tag{9}$$

In Fig. 4, we assume that $x_T = 175$ and $\alpha = \frac{50}{400} = \frac{1}{8}$. Then any (c, d) combinations that satisfy Eq. (9) can be used for desired utility function curve of Eq. (8). In our simulation study we used $c = 30$ and $d = 40$. If the threshold is changed, then the sensing utility value from each UAV can be different. However, because the proposed method derives optimal UAV

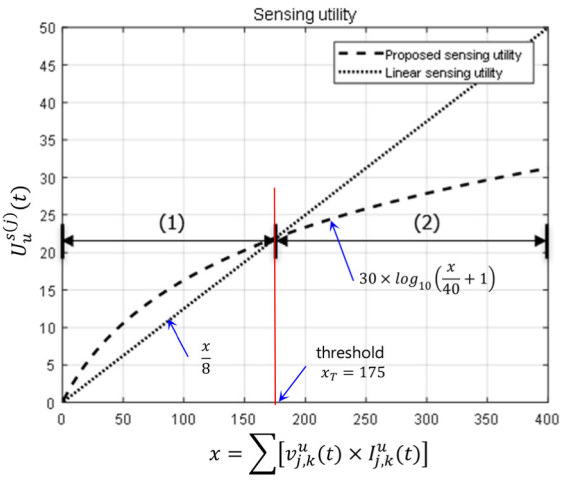

FIGURE 4. Comparison of proposed sensing utility function with the linear function.

positions that maximize the total utility, the tendency of the performance analysis result remains unchanged.

Fig. 4 shows a comparison of the proposed sensing utility function $U_u^{s(j)}(t)$ with a simple linear function, with respect to the increase in the value of $\sum_{k=1}^{N_j^u(t)}\left[v_{j,k}^u(t) \times I_{j,k}^u(t)\right]$. As shown in Fig. 4, in region (1), when the acquired VSI of a certain type of sensors is less than the predetermined threshold, the proposed sensing utility function makes the value higher than that with the linear function. Meanwhile, when the acquired VSI is higher than the threshold, the proposed function makes the value smaller than that with the linear function, as in region (2) of Fig. 4.

C. COMMUNICATION PATH QUALITY UTILITY

During the transmission and reception of sensing data in WSNs, packet errors can occur depending on the quality of each link on the path from a sensor node to the GBS. Links can be defined as either "between a sensor and a UAV", "between UAVs.", or "between a UAV and GBS". In this paper, the link quality is represented by the packet transmission success ratio. If we locate UAVs in the positions that provide better link qualities, we can acquire sensing data of sensors at the GBS more reliably. Link quality is affected by the communication channel between the transmitter and the receiver. Recently, various studies have been made on the channel model between UAVs and between UAV and ground devices [26]. Navuday Sharma *et al.* extracted the main parameters (path loss exponent and the standard deviation of the shadowing) used in the channel models and the Line of Sight (LoS)/Non Line of Sight (NLoS) probabilities as a function of the transmitter height and elevation angle using a commercial 3D ray-tracing simulator [27]. Bae *et al.* [28] presented the research results on multipath channels and mobility influences in UAV based broadcasting, in which they combined the Rayleigh and Rician channel criterion with the multipath channel profiles of DVB-T2. Depending on the operation conditions such as urban/rural

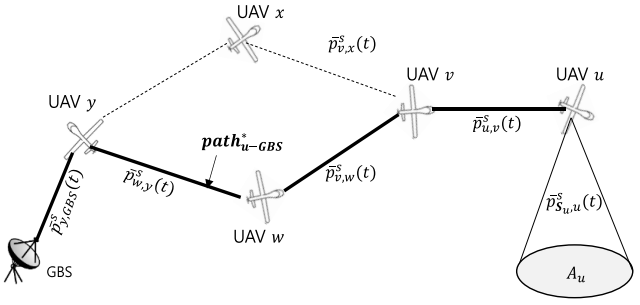

FIGURE 5. Likely sensing-data delivery paths from sensors to ground base station.

area and LoS/NLoS, different channel models can be applied, including Rician and Rayleigh models. A detailed UAV channel model study is out of the scope of this paper.

In [29], the average packet error rate (PER) over a Rayleigh fading channel, $\bar{p}_E(\bar{\gamma})$ is computed as:

$$\bar{p}_E(\bar{\gamma}) = 1 - e^{-\frac{a_N}{\bar{\gamma}}}\Gamma\left(1+\frac{b_N}{\bar{\gamma}}\right) \tag{10}$$

$$a_N = \frac{\log_{10}(N \times c_m)}{k_m}, b_N = \frac{1}{k_m} \tag{11}$$

where $\bar{\gamma}$ is the average signal-to-noise ratio (SNR); $\Gamma(\cdot)$ is the standard gamma function; N is the packet length in bits; c_m and k_m are the modulation specific constants, with values according to the modulation methods (e.g., for FSK $c_m = 1/2$ and $k_m = 1/2$; for BPSK $c_m = 1$ and $k_m = 2$). For a specified transmission power, the average SNR in a UAV-based network in free space depends mainly on the distance between the communication pair. In this paper, we assume that the average SNR between the sensors and a UAV and among the UAVs can be estimated when the locations of the UAVs are specified.

In a UAV-based network, when there is a packet error, re-transmission can be performed. When the maximum transmission counter for a packet is Q, the average packet transmission success rate over the link between nodes u and v at time t, $\bar{P}_{u,v}^{S}(t)$, is computed as:

$$\bar{P}_{u,v}^{S}(t) = 1 - \left\{\bar{p}_E\left(\bar{\gamma}_{u,v}(t)\right)\right\}^{Q} \tag{12}$$

where $\bar{\gamma}_{u,v}(t)$ is the average SNR between node u and v at time t. The node pair (u,v) can be "sensor and UAV", "UAV and UAV" or "UAV and GBS".

Fig. 5 shows the sensing data delivery paths from the sensors within the sensing area of UAV u to the GBS. Any routing algorithm can be used to deliver the sensing data acquired from UAV u to the GBS. In this study, we use the path, $path_{u-GBS}^{*}(t)$, as the optimum routing; it maximizes the successful packet-delivery rate from UAV u to the GBS at t as follow:

$$path_{u-GBS}^{*}(t) = arg \max_{path_{u-GBS}(t)} \prod_{(v,w)\in path_{u-GBS}(t)} \bar{P}_{v,w}^{S}(t) \tag{13}$$

Finally, the communication-path-quality utility of UAV u is determined as in (14); it represents the successful-packet-delivery rate from the sensors within the area of UAV u to

the GBS:

$$U_u^P(t) = \left[1 - \left\{\bar{p}_E\left(\bar{\gamma}_{\boldsymbol{S_u},u}(t)\right)\right\}^Q\right] \prod_{(v,w)\in path^*_{u-GBS}(t)} \times \left[1 - \left\{\bar{p}_E\left(\bar{\gamma}_{v,w}(t)\right)\right\}^Q\right] \quad (14)$$

where $\bar{\gamma}_{S,u}(t)$is the average SNR of the links between UAV u and the set of sensors $\boldsymbol{S_u}$ within the area of UAV u. Packet length effects on the average packet error rate (PER) as in Eq. (10) and it impacts on the link quality between UAVs or between UAV and sensors. As shown in Eq. (10), the larger packet length results in the higher PER so that finally the communication path quality utility of Eq. (14) will decrease.

D. NETWORK CONNECTIVITY UTILITY

In WSNs, the sensing data should be delivered to the GBS (or sink node) within an appropriate time. Therefore, although UAVs may successfully acquire sensing data from sensors, if they cannot connect from the UAV FANET to the GBS, the sensing data may be inconsequential. For specified UAV positions at time t, for a pair of UAVs u and v, the connectivity index $C_{u,v}(t)$ is determined as in (15):

$$C_{u,v}(t) = \begin{cases} 1, & d_{u,v}(t) \le d_{U-U}^{max} \\ 0, & else \end{cases} \quad (15)$$

where d_{U-U}^{max} is the maximum communication range between UAVs. To decode the signal transmitted from other UAVs, the received signal strength should be equal to or higher than the minimum decodable power of a UAV ($P_r^{U,min}$). Because UAV-to-UAV communication is performed in free space, d_{U-U}^{max} can be calculated as:

$$d_{U-U}^{max} = \sqrt{\frac{G_t^U \times G_r^U \times \lambda_S^2 \times P_t^U}{(4\pi)^2 \times P_r^{U,min}}} \quad (16)$$

where G_t^U, G_r^U, λ_U and P_t^U represent the transmit antenna gain, receive antenna gain, wavelength and transmission power, respectively, of a UAV.

From the GBS, if we sequentially connect UAVs with connectivity index one, we can construct a mesh-type UAV network topology. Finally, the network connectivity utility of UAV u at time t can be represented as:

$$U_u^C(t) = \prod_{\forall_{(v,w)\in path^*_{u-GBS}(t)}} C_{v,w}(t) \quad (17)$$

E. TOTAL UTILITY

In this study, to determine the optimum positions of all the UAVs at time t, we have defined the total utility function as in (18); herein, the sensing utility, communication path utility, and network connectivity utility of each UAV are considered:

$$U^T(t) = \sum_{u=1}^{N_U} U_u^S(t) \times U_u^P(t) \times U_u^C(t) \quad (18)$$

where N_U is the number of UAVs.

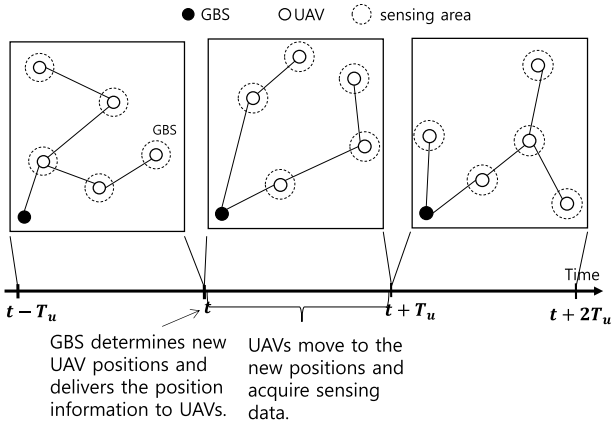

FIGURE 6. Updating the optimum uav positions and sensing data delivery using dynamic uav networks.

Fig. 6 shows the overall UAV-assisted sensor network operation. At the GBS, all the acquired sensing data is integrated and analyzed. Based on the acquired data, the GBS updates the VSIs of the sensors in the sensor field. After a predefined position update interval, T_u, the GBS determines the next UAV positions that can maximize the total utility (as expressed in (18)). As shown in Fig. 6, at time t, the GBS derives the new optimum UAV positions and delivers the position information to each UAV through the UAV FANET that was constructed at $(t - T_u)$. When the UAVs receive the new-position information at time t, they move to the indicated positions and start to acquire the sensing data from the sensors in each UAV sensing area. The acquired sensing information is delivered to the GBS through the updated UAV FANET network topology.

V. PSO-BASED UAV POSITIONING OPTIMIZATION

In this section, we propose a PSO-based multiple-UAV positioning algorithm that can maximize the proposed total utility at each position-update time. PSO is capable of iteratively searching the global optimum for large and complex spaces and has the advantage of shorter convergence time. In a WSN field, when the number of UAVs is N_U and the size of the sensor area is $(N \times M)$ unit size, the number of sets of feasible positions of multiple UAVs required to search is $(N \times M)^{N_U}$. The PSO algorithm optimizes the problem by using sets of candidate UAV locations called particles. A swarm of particles that represent potential solutions are evolved in the search space, and each of them has its position, velocity, and fitness value. A particle moves to the next position using the best position the particle has experienced and the best position that all the particles have experienced; moreover, the PSO algorithm solves the optimization problem by iteratively updating particles [30]–[32].

To determine the optimal solution, each particle adjusts its flight according to its own flying experience and companion's flying experience. A swarm of particles is developed, and the initial particles are randomly generated in the search space. Particles retain their best positions in their memory. We should ensure that all the particles stay inside

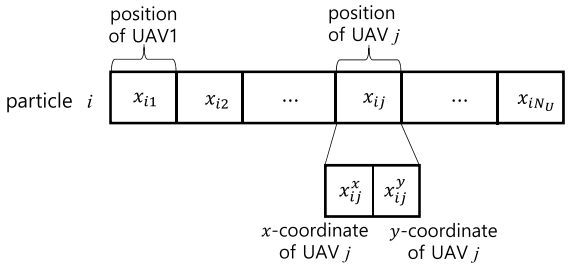

FIGURE 7. Particle structure of proposed PSO algorithm.

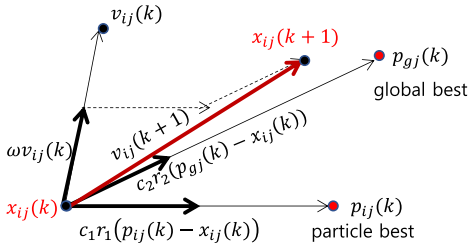

FIGURE 8. PSO convergence toward optimum solution.

the search space. If a particle is outside the search space, it is moved back inside randomly. Finally, it is compelled to stay at the border. Based on its searching mechanism, the primitive position denotes the solution, and the velocity denotes the mutative direction the solution may adopt.

The particle of the proposed PSO algorithm represents the positions of the multiple-UAVs at each UAV-position-update time. Fig. 7 shows the structure of particle i. A particle is a candidate position of multiple-UAVs, and a UAV position is represented by a certain point (x and y coordinates) in the sensor field. In a D-tuple searching space, the position and velocity of particle i are denoted by $X_i = [x_{i1}, x_{i2}, \cdots, x_{iN_U}]$ and $V_i = [v_{i1}, v_{i2}, \cdots, v_{iN_U}]$, respectively. x_{ij} represents the position of the j-th UAV for the i-th particle; $\left(x_{ij}^x, x_{ij}^y\right)$ represents the x and y coordinates of the UAV. Our fitness function is for evaluating each particle to determine the local best solution $P_i = [p_{i1}, p_{i2}, \cdots, p_{iN_U}]$. The PSO algorithm can also be used to determine the global best optimum solution $P_g = [p_{g1}, p_{g2}, \cdots, p_{gN_U}]$ that maximizes the total utility (equation (18)). The velocity and position of the j-th UAV of particle i are updated as in (19) and (20), respectively, until the total utility converges or the PSO iteration count k attains a predefined number.

$$v_{ij}(k+1) = \omega v_{ij}(k) + c_1 r_1 \left[p_{ij}(k) - x_{ij}(k)\right] + c_2 r_2 \left[p_{gj}(k) - x_{ij}(k)\right] \quad (19)$$

$$x_{ij}(k+1) = x_{ij}(k) + v_{ij}(k+1), \quad j = 1, \cdots, N_U \quad (20)$$

where ω denotes the inertia weight factor. $\{c_1$ and $c_2\}$ are position acceleration constants, and $\{r_1$ and $r_2\}$ are random numbers uniformly distributed in the interval [0, 1]. The role of ω is to regulate the impact of the previous history of velocity on the current velocity; this is considered to be crucial for convergence. Thus, it regulates the tradeoff between the global and local exploration for the swarm. A large ω causes the searching to escape from the local minima and facilitates global searching; meanwhile, a small ω facilitates local searching and convergence. When the particles are entrapped in the local optima, the inertia weight is augmented. Meanwhile, when they are dispersive, the weight is decreased. In PSO optimization, two search components (exploration and exploitation) have to be balanced. Exploration is needed for the swarm to search the whole space roughly whereas exploitation is the focusing on certain potentially good areas. With the asymptotic statistical analysis [33], to converge the optimal value, criteria to be satisfied are $-1 < \omega < 1$, $c_1 + c_2 < 4(1+\omega)$. Depending on the objective function, different optimum values for (ω, c_1, c_2) are obtained. Literature suggests several different ranges, $\omega = (0.5 \sim 0.75)$, $(c_1, c_2) = (0.9 \sim 1.7)$. The velocity interval $[v_{min}, v_{max}]$ and UAV position range $([x_{min}, x_{max}], [y_{min}, y_{max}])$ are to limit the searching to the required domain. The above velocity renewal in (19) comprises three parts.

The first part is dominated by the current velocity and contributes to the tradeoff between the global searching and local searching; meanwhile, the second part embodies a cognitive pattern and is to adjust the direction based on its recollection to prevent local minima. The third part reflects the social effects that the shared information contributes to the collaboration. The PSO convergence toward the optimum best solution is illustrated in Fig. 8.

Algorithm 1 illustrates the overall procedure of the proposed optimal UAV positioning method using PSO. After UAVs move to the optimum positions (line 1), they acquire sensing data from sensors located inside the each UAV sensing area (line2) and the information is delivered to the GBS using the optimum UAV FANET routing path computed as in Eq. (13) (line3). If UAV position update time is attained, then the GBS derives the new optimum UAV positions using PSO algorithm after updating VSI values of sensors. For each particle, based on the total utility function of Eq. (5) of the current PSO iteration time, particle's local best and global best are stored (line 6-16). If the PSO iteration number is greater than predetermined max or the difference of the total utility from the previous one is less than the threshold ε, then PSO is terminated (line 6). The new UAV position information is delivered to all the UAVs using the current FANET network (line 20) and the UAVs move to their new positions.

VI. SIMULATION RESULTS

In this section, we evaluate and analyze the performance of the proposed optimal UAV positioning mechanism. First, we evaluate the convergence performance and graphical UAV positioning procedure. Then, we describe a comparison of the obtained utility with other methods. Table 1 lists the parameters and values used in this simulation study. The sensors were deployed in the sensor field in several geo-locational clusters; herein, the cluster centers are randomly selected, and in a cluster, sensors are deployed with Gaussian distribution.

We implemented the UAV-assisted sensor network simulator using the MATLAB GUI (Fig. 9). The simulator can

Algorithm 1 Proposed UAV Positioning Method Using PSO

1: UAVs move to the (new) optimum positions.
2: UAVs maintain the proper altitude h and acquire sensing data from the sensors within each UAV sensing area A_U.
3: The sensing data acquired by each UAV u is delivered to the GBS using the optimum routing path $path^*_{u-GBS}(t)$
4: ***if*** (UAV position update interval T_U is attained.)
5: GBS updates the VSI of the sensors in the entire sensor field based on their sensing history using Eq. (5).
/* Perform the following PSO algorithm to derive the next optimum positions of the multiple UAVs. */
6: ***while*** (iteration $k \leq$ max or $\left|U^T(k) - U^T(k-1)\right| \geq \varepsilon$)
7: ***for*** (each particle i of the swarm)
8: calculate the total utility function (Eq. (18));
9: ***if***($U^T(k)$ of particle $i >$ local best of the particle)
10: local best $P_i =$ the current position of the particle;
11: ***end if***
12: ***if***($U^T(k)$ of particle $i >$ global best of the swarm)
13: global best $P_g =$ the current position of the particle;
14: ***end if***
15: update velocity and position of particle i;
16: ***end for***
17: increase iteration number $k = k+1$;
18: ***end while***
19: ***end if***
20: GBS delivers the new UAV position information to all the UAVs using the current UAV ad-hoc network.
20: Go to step 1;

import 3D maps and deploy the desired number of sensors in the sensor field. It also includes the PSO optimizer to derive the optimum UAV positions and UAV FANET routing protocol using equations (18) and (13). The routing algorithm used for simulation is to select a path that maximizes the successful packet-delivery rate from UAV u to GBS using Eq. (13). Once the UAV mesh network topology was constructed, a link state routing algorithm with Eq. (13) was applied.

In this simulation study, for performance comparison, we have implemented three UAV positioning methods apart from the proposed one: ''Sequential PSO'' uses the proposed utility function and PSO algorithm; however, it derives the UAV positions sequentially. ''Max sensor node position with connectivity'' computes the optimum UAV positions to maximize the number of sensors from which a UAV can acquire sensing data. ''Random position with connectivity'' locates UAVs randomly but guarantees UAV connections.

For Fig. 10∼ Fig. 16, the number of clusters is 10; the total number of sensors is 300; the UAV transmission power is 250mW; the sensor transmission power is 5mW.

TABLE 1. Simulation parameters.

Parameter	Symbol	Value
Number of UAVs	N_U	2-5
Number of sensor types	N_T	3
Sensor-field size	–	2×2 km
Number of sensors for each sensor type in a cluster	–	20-50
Number of clusters	–	6-12
Maximum VSI for each type	V_j^{max}	{10, 15, 20}
Minimum VSI for each type	V_j^{min}	{0.1, 0.15, 0.2}
VSI recovery interval	R_j	$\{3T_U, 5T_U, 7T_U\}$
UAV position update interval (unit time)	T_U	1
SNR between UAVs	$\gamma_{u,v}$	3–7 dB
SNR between UAV and sensors	$\gamma_{s_u,u}$	3–7 dB
Modulation specific constants	c_m, k_m	{0.5, 0.5}
Minimum decodable power	$P_r^{U,min}$	- 76 dBm
Antenna gain	G_t, G_r	{1, 1}
Frequency of signal	$3 \times 10^8/\lambda$	2.4 GHz
Altitude of UAVs	h	0.1 km
UAV transmission power	P_t^U	150-300 mW
Sensor transmission power	P_t^s	3-6 mW
Number of PSO particles	–	10, 30
Packet length	N	20 bits
Inertia weight of PSO	ω	0.5
Acceleration constants of PSO	c_1, c_2	{1.4, 1.4}
Sensing utility constants	c, d	{30, 40}

Before we compare the sensing information gathering performance with the three other methods, we illustrate the operation behaviors and results of the proposed method. Fig. 10 shows an example sensor network topology; herein, sensors of three types are deployed in a 2 × 2-km sensor field. The GBS is located at (0,0). Fig. 11 shows the variations in the total utility as the PSO iteration number increases for Fig. 10 sensor topology. For this simulation we used four UAVs. As is evident from Fig. 11, the total utility increases as the iteration number increases, and its value converges to the optimum after approximately 150 iterations. Furthermore, a larger PSO particle size results in a higher total utility because UAVs can then search more areas.

Fig. 12 shows the variations in the optimal positions of multiple UAVs over time. The number of UAVs is four, and the particle size of PSO is 30. The colored circles indicate the sensing area of each UAV, and the dotted lines represent the feasible communication links between UAVs or between a UAV and the GBS. Fig. 12 (a) shows the optimal locations at the initial state so that the VSI values of all the sensors in the sensor field are set to each sensor type's initial maximum values. At the second position-update time (after T_u) the PSO algorithm determines a different set of UAV locations that can maximize the proposed total utility; this is because after the first UAV positioning, the VSI values of the sensors whose sensing data has been delivered to the GBS are adjusted as in Eq. (5). As is evident in Fig. 12 (a)–(f), UAV1 is always connected to the GBS, and its sensing area is overlapped

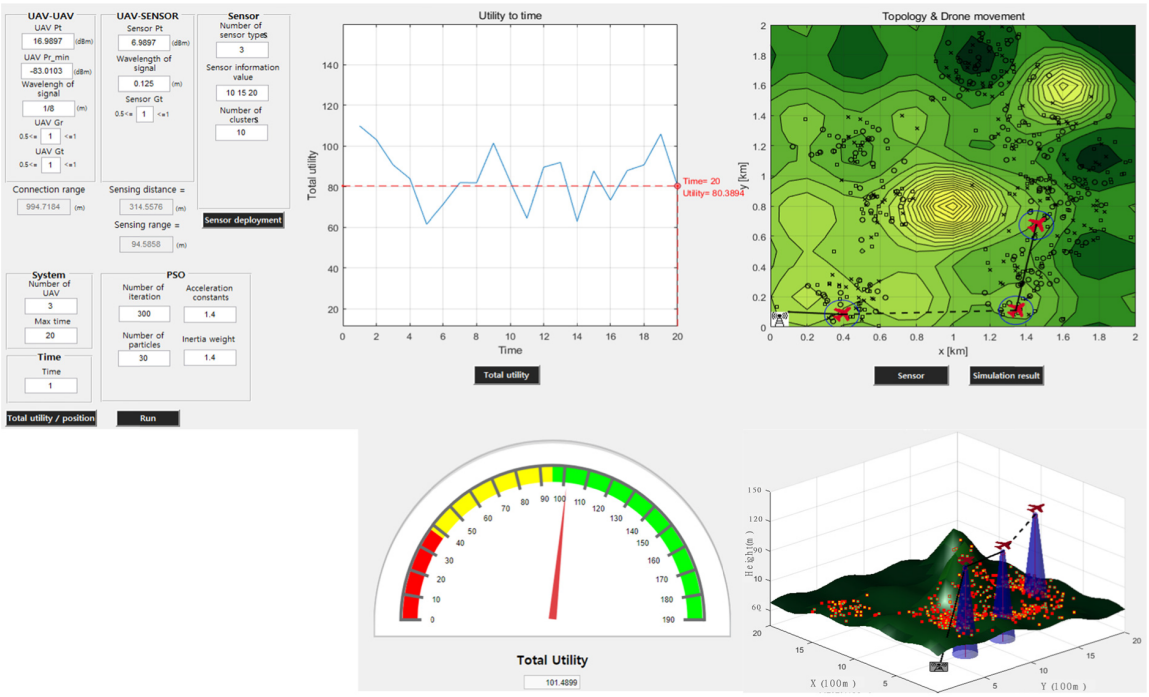

FIGURE 9. Simulator implementation.

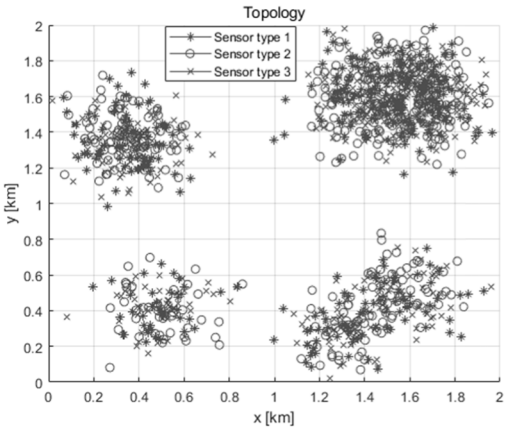

FIGURE 10. Example simulation topology.

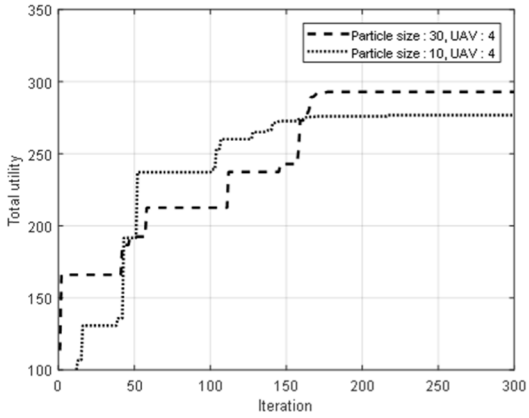

FIGURE 11. Variation in total utility with respect to PSO iterations.

with the previous ones to the least feasible extent. Fig. 12 (e) represents the optimal locations of the UAVs at the ninth position-update time. It is evident that the locations of the UAVs are similar to those of Fig. 12 (c). This is because most of the sensors that delivered their sensing data to the GBS at the third UAV-reposition time have not been covered by any UAV until the eighth UAV-reposition time, so that their VSI values are recovered to the initial values.

Fig. 13 shows the total utility variations for each UAV position update time T_u for the scenario in Fig. 12. It is observed that the total utility at the initial state (at the first positioning time) is the highest; thereafter, the total utility fluctuates accordingly. It should be noted that the total utility curve does not exhibit a periodic feature; this is because for certain updated UAV position times, a few of the sensors that were previously covered but not recovered to the initial VSI values yet, can be included again in UAV sensing areas.

The following describes a comparison of the performance of the proposed PSO method with the compared methods. In the simulation study for Fig. 14 $\sim$ Fig. 16, the number of UAVs is three, and the particle size is 30. The utility of each UAV at 10 position-update times was measured for 10 sensor deployment topologies.

As explained earlier, "Sequential PSO" is a variant version of the proposed PSO algorithm with regard to the determination of the multiple UAV-positions; the exception is that in the former, each UAV-position is determined sequentially. The location of the first UAV is the position where the total utility is the maximum by using the PSO algorithm within the area that can be connected to the GBS. Moreover, the second UAV-position is where the total utility is the

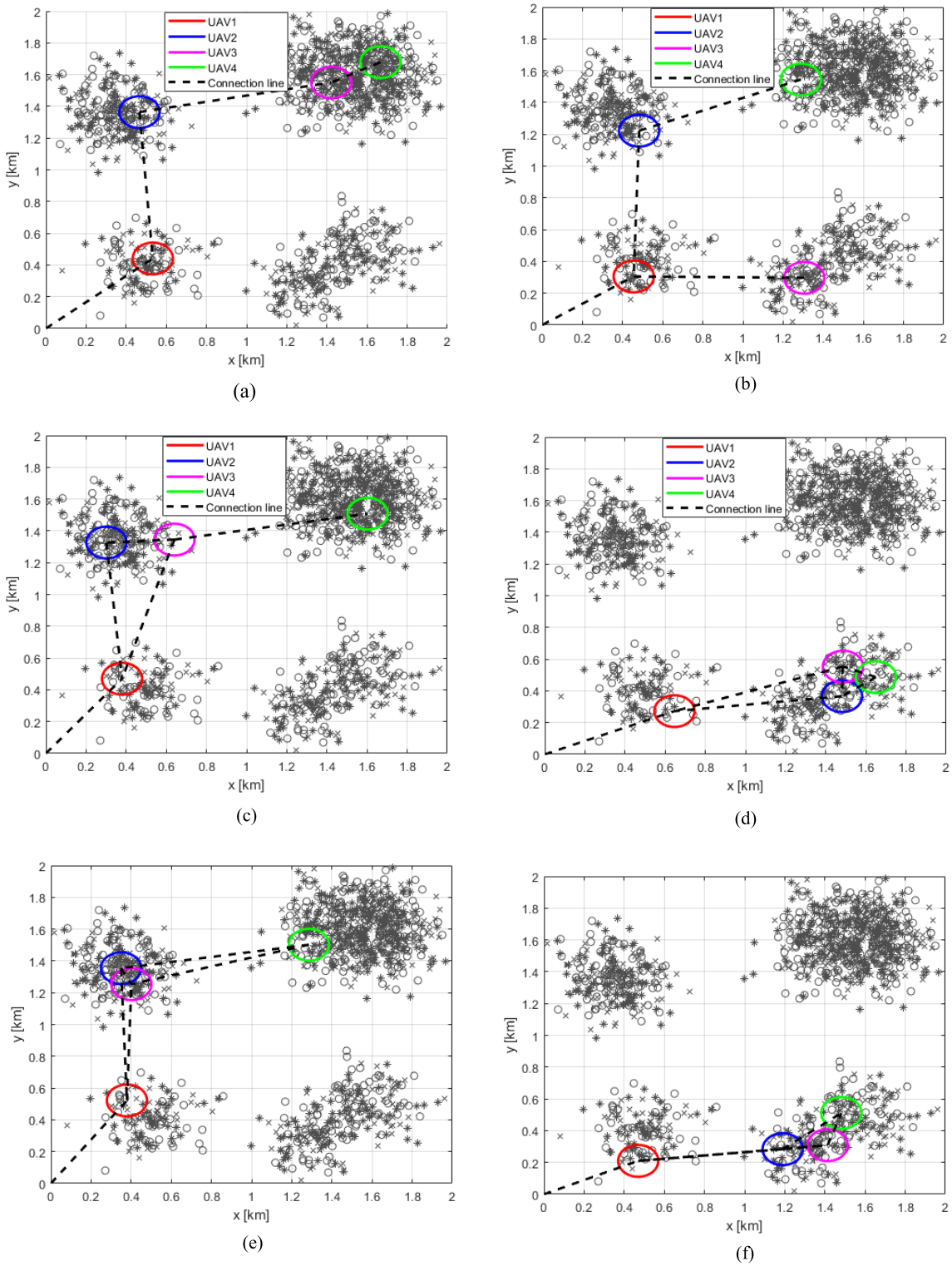

FIGURE 12. Optimum UAV positions at different update times. (a) First time. (b) Second time. (c) Third time. (d) Fourth time. (e) Ninth time. (f) Tenth time.

maximum using the PSO algorithm in the range that can be connected to the first UAV. The next UAV-position is determined similarly after the previous UAV-position is fixed. ''Max sensor node position with connectivity'' computes the optimum UAV positions to maximize the number of sensors from which the UAVs can acquire sensing data; herein, the connectivity between all the UAVs should be guaranteed. ''Random position with connectivity'' locates the UAVs

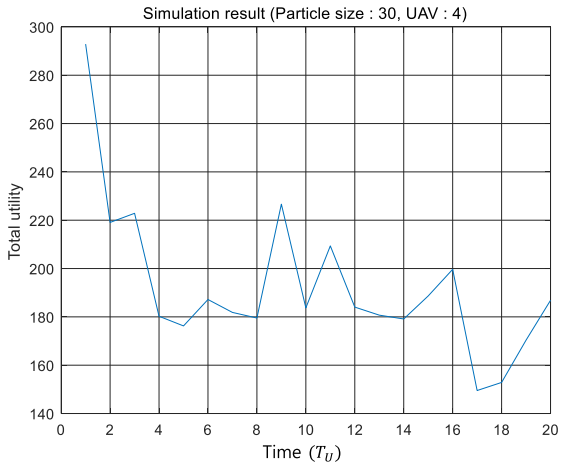

FIGURE 13. Total utility over time.

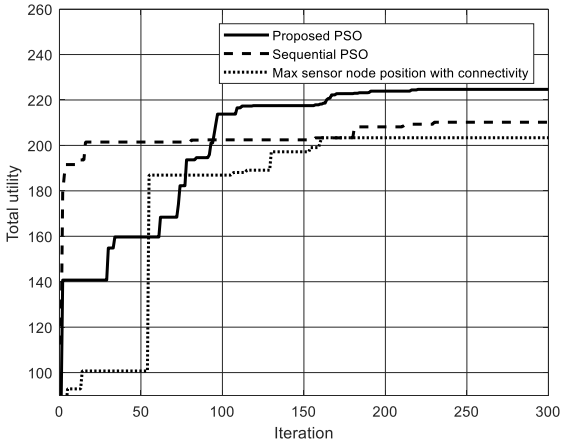

FIGURE 14. Total utility convergence comparison at initial state.

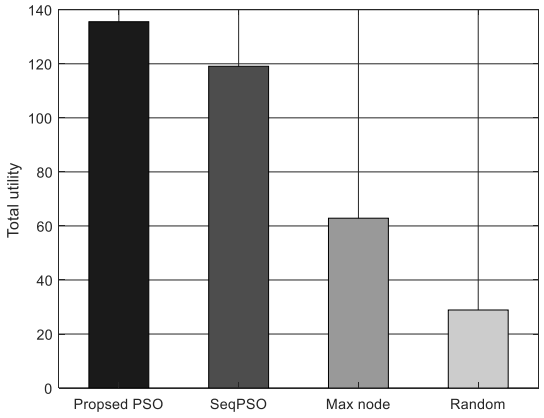

FIGURE 15. Total utility comparison.

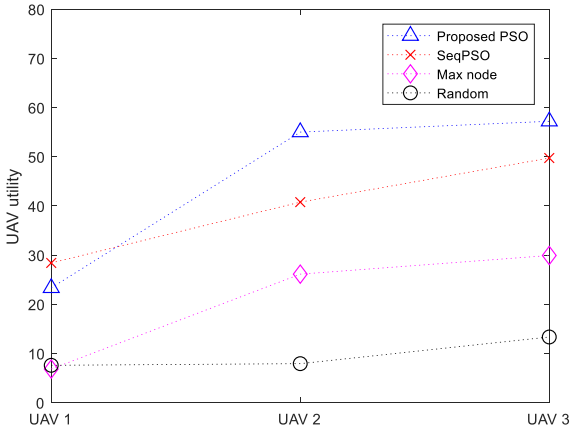

FIGURE 16. Utility comparison for each UAV.

randomly while guaranteeing their network connectivity with the GBS.

Fig. 14 shows the variation in the total utility according to the iterations at the initial state (i.e., at the first multiple-UAV positioning time). Because "Random position with connectivity" does not require PSO iterations, it is not included in this comparison. In terms of the convergence speed, "Sequential PSO" was the first to converge to a stable value. This is because in "Sequential PSO," the search area to determine the next UAV-position is limited to the communication range of the previous UAVs (or GBS). In the case of the proposed method and "Max sensor node position with connectivity" method, the search area is the entire sensor field. In terms of obtained total utility, the proposed method achieved the highest after it converged.

Fig. 15 shows the average total utility during ten position-update times. The proposed method resulted in the highest performance, whereas "Random position with connectivity" yielded the lowest utility. In "Max sensor node position with connectivity," the UAVs maintain their positions after the optimum positions for the UAVs is determined so that the VSIs of the sensors within the UAV areas decrease and are not recovered to the initial values at each T_U. In the case of "Sequential PSO", it utilizes the same optimization mechanism with the proposed method except for the UAV positions that are sequentially determined. Therefore the total utility is a little lower than that of the proposed one. As we can see in Fig. 15, the total utilities of the "Sequential PSO", "Max sensor node position with connectivity" and "Random position with connectivity" are about 91%, 33% and 24% of that of the proposed method, respectively.

Fig. 16 shows the average utility for each UAV. The proposed method generally provides higher utility for each UAV compared with other three methods. In "Sequential PSO," only the first UAV connected to the GBS obtained higher utility compared with that of the proposed method because it tries to find the first UAV position that maximizes only its utility and then sequentially determines the next UAV positions. On the other hand, the proposed method simultaneously considers all UAV positions that maximize the total utility.

For Fig. 17 $\sim$ Fig. 20, we compared the average acquired total utility by changing some simulation parameter values. The default parameter values are the same with the above simulation studies. Fig. 17 shows the average total utility for the cases having different number of UAVs. As we can see, the larger number of UAVs results in the higher acquired total utility due to the fact that UAVs could cover larger sensor network area at a given time. If there are two UAVs, the region

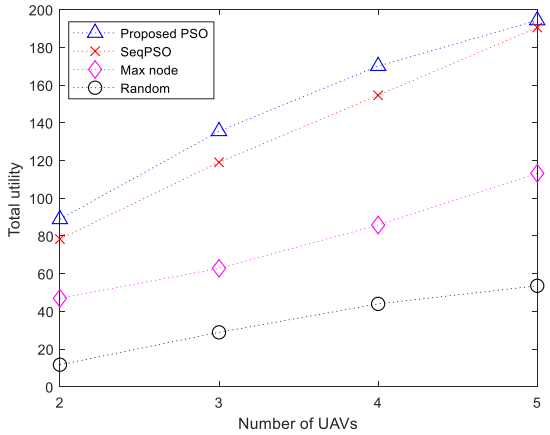

FIGURE 17. Total utility comparison for the different number of UAVs.

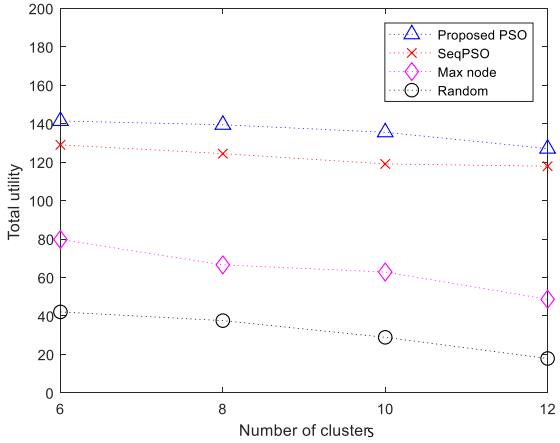

FIGURE 18. Total utility comparison for the different number of clusters.

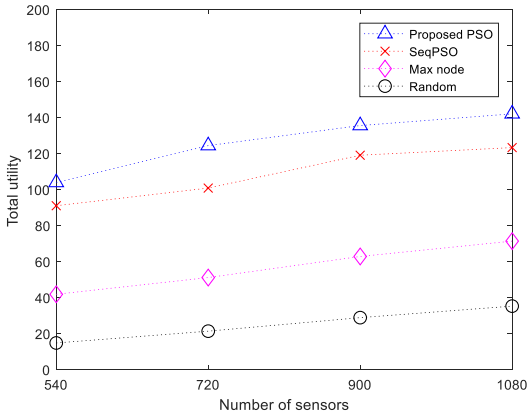

FIGURE 19. Total utility comparison for the different number of sensors.

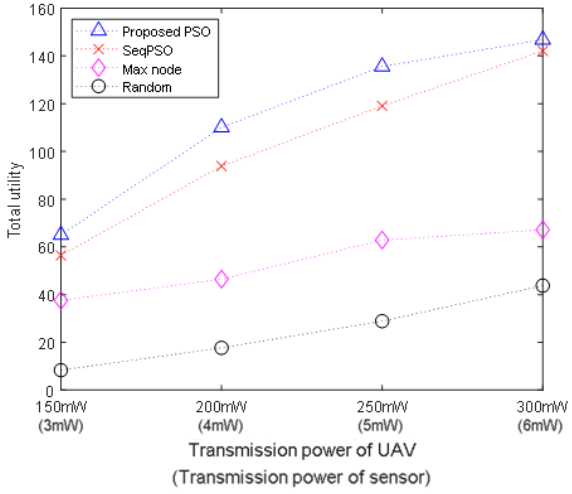

FIGURE 20. Total utility comparison for the different transmission power.

that can be searched is limited so that the total utility would be about 50% of that of four UAV case. When there are five UAVs, most areas can be searched using the proposed mechanism. Therefore, the difference between the 'Proposed PSO' and the ''Sequential PSO'' is very small. It should be noted that the 'Sequential PSO' is a simplified variant of the 'Proposed PSO'.

Fig. 18 shows the average total utility when the number of clusters is changed. In this simulation, the number of clusters is 6, 8, 10 and 12. As the total number of deployed sensors in the sensor field is the same for all cases, the larger number of clusters indicates lower sensor density in a cluster. For all compared methods, the total utility decreased as the number of clusters increased. The 'Proposed PSO' achieved the highest total utility for all different cluster sizes.

In Fig. 19, we increased the number of sensors and fixed the number of clusters to 10. The total utility increases as the number of sensors increase in all methods. However, when comparing 540 sensors with 1080 sensors, even though the number of sensors is doubled, the average acquired total utility is not. This is because the sensing utility function is not linearly proportional to the number of sensors covered by UAVs. As in Eq. (8) and Fig. 4, the sensing utility increases slowly if the acquired VSI is greater than the threshold.

In Fig. 20, we changed the transmission power of UAV and sensor. For UAV transmission power, 150mW, 200mW, 250mW and 300mW are used; for sensor transmission power 3mW, 4mW, 5mW and 6mW are used. Since higher transmission power results in longer communication distance, a UAV can get a larger sensing area. As shown in Fig. 20, if we double the transmission power of UAV and sensors (from 150mW to 300mW for UAV and from 3mW to 6mW for sensors, respectively), then the total utility is more than doubled for the 'Proposed PSO'.

VII. CONCLUSION

In this paper, we propose a PSO-based optimization algorithm to derive dynamic multiple-UAV-positions that can acquire maximum sensor data information in UAV-assisted WSNs. We first defined the VSI functions for different sensor types. The defined VSI function can express the importance of different sensor types as well as the variation in the value of the sensed data depending on the time and spatial domain redundancy. Then, we proposed the total utility function that represents the total VSI actually determined by the multiple UAVs. We considered sensing utility, communication path utility, and network connectivity utility. For the specified positions of multiple UAVs, we can compute the total VSI from the

sensor field; herein, the spatial duplication of the sensing data is removed, and successful sensing-data delivery rate on the UAV routing path and each UAV's network connectivity are considered. At each UAV-position-update time, the VSI statistics for the sensor field are updated, and the optimum next positions of the multiple UAVs are determined using the proposed PSO-based positioning algorithm. In the proposed method, there is no additional overhead such as the extra exchange of messages between sensors and UAVs to track the status of the sensor. However, it is necessary to update each VSI value at the GBS according to the proposed VSI update function based on the reporting form each sensor.

For the simulation study, we implemented a GUI-based simulator that could set various sensor network topologies and simulation conditions. We demonstrated the convergence performance of the proposed PSO algorithm and how the total acquired VSI varied over time when the UAVs changed their positions at each position-update time. We compared the performance with three other positioning methods. We have verified that the performance of the proposed algorithm is the highest in terms of total acquired utility.

In this paper, to apply the proposed PSO-based UAV positioning method, we assume that the geographical map and sensor deployment are known in advance. For the further research, we will study the cooperative UAV operations when we cannot or only partially obtain this information in advance. Currently we implement the proposed method using drones and various types of sensor in out-door sensor network test-bed and will perform additional supplement by comparing empirical results with the simulation results.

REFERENCES

[1] P. Rudol and P. Doherty, "Human body detection and geolocalization for UAV search and rescue missions using color and thermal imagery," in *Proc. IEEE Aerosp. Conf.*, Mar. 2008, pp. 1–8.
[2] C. Zhang and M. John Kovacs, "The application of small unmanned aerial systems for precision agriculture: A review," *Precis. Agricult.*, vol. 13, no. 6, pp. 693–712, Dec. 2012.
[3] S. Shen, N. Michael, and V. Kumar, "Autonomous multi-floor indoor navigation with a computationally constrained MAV," in *Proc. IEEE Int. Conf. Robot. Automat.*, May 2011, pp. 20–25.
[4] F. G. Costa, J. Ueyama, T. Braun, G. Pessin, F. S. Osório, and P. A. Vargas, "The use of unmanned aerial vehicles and wireless sensor network in agricultural applications," in *Proc. IEEE Int. Geosci. Remote Sens. Symp.*, Jul. 2012, pp. 5045–5048.
[5] R. Teguh, T. Honma, A. Usop, H. Shin, and H. Igarashi, "Detection and verification of potential peat fire using wireless sensor network and UAV," in *Proc. Int. Conf. Inf. Technol. Elect. Eng.*, Jul. 2012, pp. 6–10.
[6] M. Erdelj, M. Król, and E. Natalizio, "Wireless sensor networks and multi-UAV systems for natural disaster management," *Comput. Netw.*, vol. 124, pp. 72–86, Sep. 2017.
[7] G. Tuna, T. V. Mumcu, K. Gulez, V. C. Gungor, and H. Erturk, "Unmanned aerial vehicle-aided wireless sensor network deployment system for post-disaster monitoring," *Emerg. Intell. Comput. Technol. Appl.*, vol. 304, pp. 298–305, Jul. 2012.
[8] M. Dong, K. Ota, M. Lin, Z. Tang, S. Du, and H. Zhu, "UAV-assisted data gathering in wireless sensor networks," *J. Supercomput.*, vol. 70, no. 3, pp. 1142–1155, 2014.
[9] C. Zhang, Z. Zhen, D. Wang, and M. Li, "UAV path planning method based on ant colony optimization," in *Proc. Chin. Control Decis. Conf.*, May 2010, pp. 3790–3792.
[10] S. Mittal and K. Deb, "Three-dimensional offline path planning for UAVs using multiobjective evolutionary algorithms," in *Proc. IEEE Congr. Evol. Comput.*, vol. 7, Sep. 2007, pp. 3195–3202.
[11] M. Mishra, X. Huan, D. Sidoti, D. F. Ayala, W. An, D. L. Kleinman, and K. R. Pattipati, "Multi-objective coordinated path planning for a team of UAVS in a dynamic environment," in *Proc. 19th ICCRTS*, Jun. 2014, pp. 1–20.
[12] O. K. Sahingoz, "Flyable path planning for a multi-UAV system with genetic algorithms and Bezier curves," in *Proc. Int. Conf. Unmanned Aircr. Syst. (ICUAS)*, May 2013, pp. 41–48.
[13] D.-T. Ho, E. I. Grøtli, P. B. Sujit, T. A. Johansen, and J. B. Sousa, "Optimization of wireless sensor network and UAV data acquisition," *J. Intell. Robot. Syst.*, vol. 78, no. 1, pp. 159–179, 2015.
[14] H. Ergezer and K. Leblebicioglu, "Path planning for UAVs for maximum information collection," *IEEE Trans. Aerosp. Electron. Syst.*, vol. 49, no. 1, pp. 502–520, Jan. 2013.
[15] Q. Yang and S.-J. Yoo, "Optimal UAV path planning: Sensing data acquisition over IoT sensor networks using multi-objective bio-inspired algorithms," *IEEE Access*, vol. 6, pp. 13671–13684, 2018.
[16] S. Say, H. Inata, J. Liu, and S. Shimamoto, "Priority-based data gathering framework in UAV-assisted wireless sensor networks," *IEEE Sensors J.*, vol. 16, no. 14, pp. 5785–5794, Jul. 2016.
[17] C. Zhan, Y. Zeng, and R. Zhang, "Energy-efficient data collection in UAV enabled wireless sensor network," *IEEE Wireless Commun. Lett.*, vol. 7, no. 3, pp. 328–331, Jun. 2018.
[18] C. Zhan, Y. Zeng, and R. Zhang, "Trajectory design for distributed estimation in UAV-enabled wireless sensor network," *IEEE Trans. Veh. Technol.*, vol. 67, no. 10, pp. 10155–10159, Oct. 2018.
[19] J. Gong, T.-H. Chang, C. Shen, and X. Chen, "Flight time minimization of UAV for data collection over wireless sensor networks," *IEEE J. Sel. Areas Commun.*, vol. 36, no. 9, pp. 1942–1954, Sep. 2018.
[20] J. Sánchez-García, D. G. Reina, and S. L. Toral, "A distributed PSO-based exploration algorithm for a UAV network," *Future Gener. Comput. Syst.*, vol. 90, pp. 129–148, Jan. 2019.
[21] Q. Wang, A. Zhang, and L. Qi, "Three-dimensional path planning for UAV based on improved PSO algorithm," in *Proc. 26th Chin. Control Decis. Conf.*, May/Jun. 2014, pp. 3981–3985.
[22] X. Li, Y. Zhao, J. Zhang, and Y. Dong, "A hybrid PSO algorithm based flight path optimization for multiple agricultural UAVs," in *Proc. IEEE 28th Int. Conf. Tools Artif. Intell. (ICTAI)*, Nov. 2016, pp. 691–697.
[23] A. Al-Hourani, S. Kandeepan, and S. Lardner, "Optimal LAP altitude for maximum coverage," *IEEE Wireless Commun. Lett.*, vol. 3, no. 6, pp. 569–572, Dec. 2014.
[24] D. G. Cileo, N. Sharma, and M. Magarini, "Coverage, capacity and interference analysis for an aerial base station in different environments," in *Proc. Int. Symp. Wireless Commun. Syst. (ISWCS)*, Aug. 2017, pp. 281–286.
[25] M. C. Batistatos, G. E. Athanasiadou, D. A. Zarbouti, G. V. Tsoulos, and N. C. Sagias, "LTE ground-to-air measurements for UAV-assisted cellular networks," in *Proc. 12th Eur. Conf. Antennas Propag.*, Apr. 2018, pp. 1–5.
[26] A. A. Khuwaja, Y. Chen, N. Zhao, M.-S. Alouini, and P. Dobbins, "A survey of channel modeling for UAV communications," *IEEE Commun. Surveys Tuts.*, vol. 20, no. 4, pp. 2804–2821, 4th Quart., 2018.
[27] N. Sharma, M. Magarini, L. Dossi, L. Reggiani, and R. Nebuloni, "A study of channel model parameters for aerial base stations at 2.4 GHz in different environments," in *Proc. 15th IEEE Annu. Consum. Commun. Netw. Conf. (CCNC)*, Jan. 2018, pp. 1–6.
[28] J. Bae, Y. Kim, N. Hur, and H. M. Kim, "Study on air-to-ground multipath channel and mobility influences in UAV based broadcasting," in *Proc. Int. Conf. Inf. Commun. Technol. Converg. (ICTC)*, Oct. 2018, pp. 1534–1538.
[29] A. Mahmood and R. Jäntti, "Packet error rate analysis of uncoded schemes in block-fading channels using extreme value theory," *IEEE Commun. Lett.*, vol. 21, no. 1, pp. 208–211, Jan. 2017.
[30] Y. Feng, G.-F. Teng, A. Wang, and Y.-M. Yao, "Chaotic inertia weight in particle swarm optimization," in *Proc. 2nd Int. Conf. Innov. Comput. Inform. Control*, Sep. 2007, p. 475.
[31] S. M. A. Salehizadeh, P. Yadmellat, and M. B. Menhaj, "Local optima avoidable particle swarm optimization," in *Proc. IEEE Swarm Intell. Symp.*, Mar./Apr. 2009, pp. 16–21.
[32] R. Eberhart and J. Kennedy, "A new optimizer using particle swarm theory," in *Proc. 6th Int. Symp. Micro Mach. Hum. Sci.*, Oct. 1995, pp. 39–43.
[33] M. Jiang, Y. P. Luo, and S. Y. Yang, "Particle swarm optimization—Stochastic trajectory analysis and parameter selection," in *Swarm Intelligence: Focus on Ant and Particle Swarm Optimization*, Rijeka, Croatia: InTech, 2007.

HO JEONG NA received the B.S. degree from the Information and Communication Engineering Department, Inha University, South Korea, where he is currently pursuing the M.S. degree with the Multimedia Network Laboratory. His research interests include wireless sensor network, FANET, and machine learning.

SANG-JO YOO received the B.S. degree in electronic communication engineering from Hanyang University, Seoul, South Korea, in 1988, and the M.S. and Ph.D. degrees in electrical engineering from the Korea Advanced Institute of Science and Technology, in 1990 and 2000, respectively. From 1990 to 2001, he was a Member of Technical Staff with the Korea Telecom Research and Development Group, where he was involved in communication protocol conformance testing and network design fields. From 1994 to 1995 and from 2007 to 2008, he was a Guest Researcher with the National Institute Standards and Technology, USA. Since 2001, he has been with Inha University, where he is currently a Professor with the Information and Communication Engineering Department. His current research interests include cognitive radio network protocols, adhoc wireless network, MAC and routing protocol design, wireless network QoS, and wireless sensor networks.